

# A Stable V/f Control Method for Permanent Magnet Synchronous Motor Drives

Cheng Ajun

R&D Drive Software Dept.  
Shanghai Sigriner STEP Electric Co., Ltd  
Shanghai, China  
Chengaj@stepelevator.com

Jin Xinhai

R&D Drive Software Dept.  
Shanghai Sigriner STEP Electric Co., Ltd  
Shanghai, China  
Jinxh@stepelectric.com

**Abstract**—Permanent Magnet Synchronous Motor is characterized by high power density, high efficiency and high reliability, and it is superior in many applications. V/f control for PMSM is able to get rid of the expensive rotor position sensor, and it is of great research value. V/f control method for PMSM is investigated in this paper. Firstly, the reason for the instability of the traditional open-loop V/f control is analyzed. A speed closed-loop is introduced to avoid the instability of the system. Meanwhile, in order to enhance the efficiency of the system, a reactive power closed-loop is proposed, which is added to the system. Finally, experimental results are provided to validate the effectiveness of the proposed V/f control method.

**Keywords**—permanent-magnet synchronous motor; V/f control; stable control; Efficient control

## I. INTRODUCTION

Permanent Magnet Synchronous Motor has the characteristics of simple structure, small volume, low loss, high efficiency and high reliability. However, it is difficult to control a synchronous motor because it is necessary to determine the initial position of the encoder and therefore, it is usually used in the high precision case. It is not suitable for general applications such as a fan pump because of the cost of the position sensor. V/f control is an effective way for general applications. With the help of V/f control, the rotor position sensor is able to be saved, the cost of the system is reduced, and the reliability is improved.

In order to realize the simple control scheme similar to the one for the asynchronous motor, some scholars have studied the V/f control method of the PMSM. In [1], the stability of the system is analyzed, and the stator resistance compensation is adopted to elevate the efficiency of the system. In this method, only the stator resistance parameter is needed. In [2], the voltage is compensated according to the reactive power. And both the voltage and the angle of the current vector are compensated in [3]. The efficiency of the system is improved through controlling the power factor angle in [4~6]. By these methods, the parameters of the motor is not required and the system works well at heavy load in both the motor and generate modes. But the operating at light load is an challenge for these methods.  $i_d = 0$  method is used as the efficient control method in [7], while MTPA method is adopted in [8~11].  $i_d = 0$  method is suitable for SPM, in which the

parameter of the inductance is demanded. And MTPA method is suitable for IPM, in which the parameter of the back EMF is required except the parameter of the inductance.

In this paper, the stability of V/f control for PMSM is analyzed at first. Then the control method characterized by high stability and efficiency is proposed. And the approach to decrease the influence of the dead time compensation at light load is also introduced. At last, the feasibility of the method is validated through experimental results.

## II. CONTROL METHOD AND STABILITY ANALYSIS

### A. Analysis of PMSM Stability

If the oscillation is not be suppressed with particular methods, open-loop control of a PMSM is not a stable system [1]. Fig. 1 shows that a 25kW 195Hz motor adopting V/f control without stable loop is operated at 35Hz at no-load. The current waveform is oscillating, and at last the over-current error occurs. The simulation of the result is shown in Fig. 2, it can be clearly seen that if no stable loop is applied, the motor speed will gradually oscillate too. If the stable loop is added, the motor speed oscillation will be gradually reduced, and finally converge at a given speed.

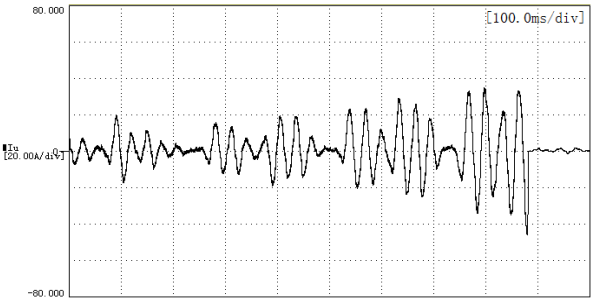
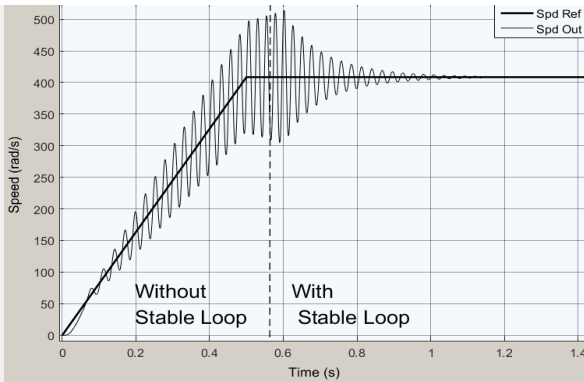


Fig. 1. No-load currents with and without stable loop.

In general, small-signal analysis can be used to analyze the stability of the system. The voltage equation for the motor is as follows

$$\begin{cases} u_d = R_s i_d + L_d \frac{di_d}{dt} - \omega_r L_q i_q \\ u_q = R_s i_q + \omega_r L_d i_d + L_q \frac{di_q}{dt} + \omega_r \psi_m \end{cases} . \quad (1)$$



Simulation of the speed with and without stable loop.

Stator flux linkage equation is

$$\begin{cases} \psi_d = \psi_m + L_d i_d \\ \psi_q = L_q i_q \end{cases} . \quad (2)$$

Electromagnetic torque equation is

$$T_e = 1.5n_p(\psi_d i_q - \psi_q i_d) . \quad (3)$$

Substitute the  $\psi_d$ ,  $\psi_q$  to torque equation

$$T_e = 1.5n_p(\psi_m i_q + (L_d - L_q)i_q i_d) . \quad (4)$$

Motion equation is

$$T_e = \frac{J}{n_p} p\omega_r + T_L + k_f \frac{\omega_r}{n_p} . \quad (5)$$

If the angle  $\delta$  is used to represent the relationship between the electrical angle and the rotor angle, then

$$\delta = \theta_e - \theta_r . \quad (6)$$

In this way,  $u_d$  and  $u_q$  can be represented by the function of  $\delta$

$$\begin{cases} u_d = -u_s \sin \delta \\ u_q = u_s \cos \delta \end{cases} . \quad (7)$$

Combining (1), (7), and (3) to (5), then

$$\begin{cases} -u_s \sin \delta = (r_s + pL_d)i_d - \omega_r L_q i_q \\ u_s \cos \delta = \omega_r L_d i_d + (r_s + pL_q)i_q + \omega_r \psi_f \\ 1.5n_p(\psi_m i_q + (L_d - L_q)i_q i_d) = \frac{J}{n_p} p\omega_r + T_L + k_f \frac{\omega_r}{n_p} \end{cases} . \quad (8)$$

Equation (6) and (8) expressed in the form of linear equations

$$\begin{cases} pi_d = -\frac{i_d}{\tau_s} + \sigma\omega_r i_q - \frac{u_s \sin \delta}{L_d} \\ pi_q = -\frac{i_q}{\sigma\tau_s} - \frac{\omega_r}{\sigma} \left( \frac{\psi_m}{L_d} + i_d \right) + \frac{u_s \cos \delta}{\sigma L_d} \\ p\omega_r = \frac{3n_p^2}{2J} (\psi_m i_q + L_d(1-\sigma)i_q i_d) - \frac{k_f \omega_r}{J} - \frac{n_p T_L}{J} \\ p\delta = \omega_e - \omega_r \end{cases} . \quad (9)$$

In(1)~(9)

$$\tau_s = \frac{L_d}{r_s}, \sigma = \frac{L_q}{L_d} . \quad (10)$$

$i_d, i_q$	Rotor d-axis and q-axis currents
$L_d, L_q$	Rotor d-axis and q-axis inductances
$p$	Operator d/dt
$\omega_r$	Electrical rotor speed
$\omega_e$	Electrical speed of the applied voltage vector
$\delta$	Load angle
$J$	Inertia of the motor and the load system
$B_m$	Viscous friction coefficient
$n_p$	Number of poles of the motor
$T_L$	Load torque

In the steady state, the differential items are 0. In small signal analysis for (9), ignoring the second sub-small, the motor characteristic equation is

$$p \begin{pmatrix} \Delta i_d \\ \Delta i_q \\ \Delta \delta \end{pmatrix} = \begin{pmatrix} -\frac{1}{\tau_s} & \sigma \omega_0 & \sigma i_{q0} & \frac{u_{s0} \cos \delta_0}{L_d} \\ \frac{\omega_0}{\sigma} & -\frac{1}{\sigma \tau_s} & -\frac{1}{\sigma} \left( \frac{\psi_m}{L_d} + i_{d0} \right) & \frac{u_{s0} \sin \delta_0}{L_d \sigma} \\ \frac{3n_p^2}{2J} L_d (1-\sigma) i_{q0} & \frac{3n_p^2}{2J} [\psi_m + L_d(1-\sigma)i_{d0}] & -\frac{K_f}{J} & 0 \\ 0 & 0 & -1 & 0 \end{pmatrix} \begin{pmatrix} \Delta i_d \\ \Delta i_q \\ \Delta \delta \end{pmatrix} + \begin{pmatrix} 0 \\ 0 \\ \frac{n_p}{J} \end{pmatrix} \Delta T_L . \quad (11)$$

The state transition matrix for this system is

$$A = \begin{bmatrix} -\frac{1}{\tau_s} & \sigma \omega_{r0} & \sigma i_{q0} & -\frac{u_{s0} \cos \delta_0}{L_d} \\ -\frac{\omega_{r0}}{\sigma} & -\frac{1}{\sigma \tau_s} & -\frac{1}{\sigma} \left( \frac{\psi_m}{L_d} + i_{d0} \right) & -\frac{u_{s0} \sin \delta_0}{L_d \sigma} \\ \frac{3n_p^2}{2J} L_d (1-\sigma) i_{q0} & \frac{3n_p^2}{2J} [\psi_m + L_d(1-\sigma)i_{d0}] & -\frac{K_f}{J} & 0 \\ 0 & 0 & -1 & 0 \end{bmatrix} . \quad (12)$$

According to the judgment condition of stability, if the eigenvalues of the state transition matrix shown in (12) are on the left half plane, the system is stable. If there are some eigenvalues on the imaginary axis, the other eigenvalues are left half plane, then the system is critical stable. Otherwise the system is unstable.

The root trajectory of the 25kW motor is shown in Fig. 3.

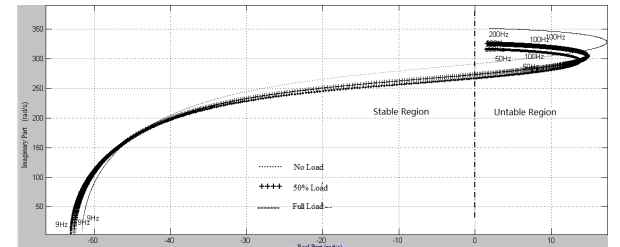


Fig. 2. Root trajectory of 195Hz 25kW motor system without stable loop.

It can be seen that in the traditional V / f control mode, the part of the eigenvalues of the system are in the right half plane, whether under no load or the full load condition. So the system is unstable.

### B. Stable V/f control of PMSM

The motor speed is not correctly estimated, which is the main reason for the unstable control of the system. If the changes of the speed is indicated through a measurable

parameter related to the speed, a stable loop is able to be established.

Since the real speed signal can't be obtained directly, it is necessary to deduce the speed information from other measurable variables. The energy balance equation of the motor is

$$\begin{aligned} p_e &= P_e + \Delta p_e \\ &= P_{ml} + \frac{dw_{em}}{dt} + \left(\frac{2}{n}\right)^2 \frac{J}{2} \frac{d\omega_r^2}{dt} + \left(\frac{2}{n}\right)^2 Br \cdot \omega_r^2 + \frac{2}{n} \omega_r T_L. \end{aligned} \quad (13)$$

In the small signal model, it can be approximated by

$$\Delta p_e = \left(\frac{2}{n}\right)^2 J \omega_0 \frac{d}{dt} \Delta \omega_r + 2 \left(\frac{2}{n}\right)^2 Br \cdot \omega_0 \Delta \omega_r + \frac{2}{n} T_{L0} \Delta \omega_r. \quad (14)$$

where,  $P_e$  is the steady-state operating speed,  $p_e$  is the offset,  $P_{ml}$  is the loss power of the motor,  $w_{em}$  is the magnetic field energy in the motor,  $\omega_0$  is the steady-state speed,  $T_{L0}$  is the static load.

Equation (14) shows that the increment of the rotor speed is proportional to the motor power, so

$$\Delta \omega_e = -k_p \Delta p_e. \quad (15)$$

where the motor power offset  $\Delta p_e$  can be obtained by the instantaneous active power of the motor

$$\Delta p_e = \frac{3}{2} \Delta(u_d i_d + u_q i_q) = \frac{3}{2} \cdot \text{HPF}(u_d i_d + u_q i_q). \quad (16)$$

The cut-off frequency of the high-pass filter in the formula needs to be adjusted according to the specific motor parameters.

After the compensation in (16) is added to the V/f control, the root trajectory is shown as Fig. 4. It can be seen that whether it is no load or full load, the eigenvalues of the system are on the left half plane after the V/f control with the stability algorithm is applied.

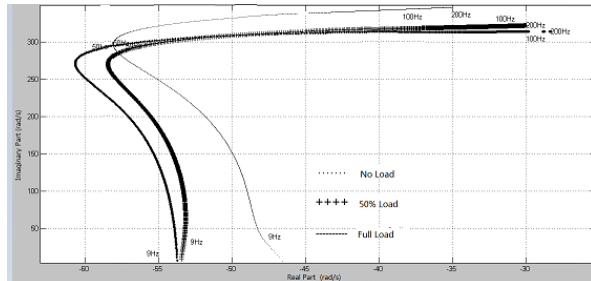


Fig. 3. Root trajectory of 195Hz 25kW motor system with stable loop.

### C. Efficient V/f control of PMSM

PMSM has stator resistance too. Voltage drop on the stator resistance will be increased when the load becomes heavier. The air-gap flux linkage decreases, which leads to the decrease of the torque. The load-drive capacity of the system is weaker and it is possible that the system becomes out of step. Therefore, a voltage compensation should be added to eliminate the voltage drop. But the voltage compensation should not be too large, or else the load capacity and efficiency of the system will be reduced. Thus it is crucial to

find an appropriate voltage compensation method in order to realize the efficient V/f control.

Previously, the voltage compensation methods are stator resistance compensation,  $i_d = 0$  compensation, MTPA compensation and power factor of 1 compensation. MTPA compensation is adopted in this paper. And it is necessary to known certain parameters of the motor, such as the  $L_d$ ,  $L_q$  and  $\psi_m$ . In the following part, the self-tuning method of the motor parameters is introduced firstly, and then the MTPA efficient control method is explained.

#### 1) estimation of the Required parameter

##### a) Stator resistance

According to Ohm's law  $R = U / I$ , the stator resistance of the motor can be measured by DC voltammetry. Because the IGBT transistor can't turn on for a long time, the equivalent DC voltage is used for the pulse voltage of fixed duty ratio. The stator current can be controlled to a specific value by the current control closed-loop, and the corresponding voltage can be calculated through the PWM duty. Then the R is able to be calculated by Ohm's law.

##### b) Back EMF

According to (1),  $i_d$  and  $i_q$  are small at no load. If the motor is running at low speed, it can be considered as  $u_d = 0$ , and all the voltage is applied to the q-axis.

The motor runs to 20Hz at no-load, and the RMS of the current reference is set to be 5% of the rated current. Then the back EMF equals to the output of the q-axis current controller plus the voltage reference.

According to (17), flux can be calculated as

$$\psi_m = \sqrt{\frac{2}{3}} \frac{V_s}{\omega_r}. \quad (17)$$

##### c) $L_d$ and $L_q$

According to (1) and (17), when  $i_d$  and  $i_q$  are set to be 80% and 10% of the rated current respectively with the help of d-axis and q-axis current control loops, and the motor is running at 20Hz, the  $L_d$  and  $L_q$  can be calculated by (18) in steady state.

$$\begin{cases} L_q = \frac{R_s i_d - u_d}{\omega_r i_q} \\ L_d = \frac{u_q - R_s i_q - \omega_r \psi_m}{\omega_r i_d} \end{cases} \quad (18)$$

#### 2) MTPA algorithm

The V/f control of PMSM removes the mechanical position sensors, therefore there is no motor position information and speed information. It is necessary to control the motor in the coordinate system which is synchronously rotating with the stator voltage vector. And  $\delta\gamma$  rotating coordinate system is introduced in this paper, in which  $\delta$ -axis is aligned to the direction of the motor output voltage vector. So

$$\begin{cases} u_\gamma \equiv 0 \\ u_\delta = u_s \end{cases} \quad (19)$$

In the  $dq$  coordinate system, when the PMSM works under the stable condition, the motor reactive power is

$$Q_{dq} = \omega_r L_d i_d^2 + \omega_r \psi_f i_d + \omega_r L_q i_q^2. \quad (20)$$

In (20), if

$$i_d = -i_s \sin \beta. \quad (21)$$

So

$$i_q = i_s \cos \beta. \quad (22)$$

Then (20) can be written

$$Q_{dq} = \omega_r i_s^2 (L_d - L_q) \sin \beta^2 - \omega_r \psi_f i_s \sin \beta + \omega_r L_q i_s^2. \quad (23)$$

Add  $i_d$  and  $i_q$ , into the torque equation

$$T_e = 1.5n_p [\psi_f i_s \cos \beta - 0.5i_s^2 (L_d - L_q) \sin 2\beta]. \quad (24)$$

To make the same current under the maximum torque, required

$$\frac{dT_e}{d\beta} = 0. \quad (25)$$

and

$$\frac{dT_e^2}{d\beta^2} < 0. \quad (26)$$

It can be calculated that

$$\sin \beta = \frac{-\psi_f + \sqrt{\psi_f^2 + 8i_s^2(L_q - L_d)}}{4(L_q - L_d)i_s}. \quad (27)$$

And in the  $\delta\gamma$  coordinate system, the reactive power equation is

$$Q_{\delta\gamma} = v_\delta i_\gamma - v_\gamma i_\delta = v_\delta i_\gamma. \quad (28)$$

Use a common PI controller, the  $Q_{\delta\gamma}$  is the reference and the  $Q_{dq}$  is the feedback, the compensation voltage  $\Delta v$  is

$$\Delta v = PI(Q_{dq}, Q_{\delta\gamma}). \quad (29)$$

According (17) and (29), The final output voltage is

$$v_\delta = \sqrt{\frac{3}{2}} \omega_r \psi_m + \Delta v. \quad (30)$$

#### D. The impact of dead time on the system

In order to avoid direct connection of the leg of the inverter, it is indispensable to add the dead-zone to the complementary switching signals for the upper and lower IGBTs in the SVPWM. However, dead-zone can also cause distortion of the output current and zero-current clamp.

One of the dead-time compensation methods is to compensate the voltage. A positive voltage is added when the output current is greater than zero, and a negative voltage is added in other case. The no-load currents are so small that it is difficult to judge the direction of the current. Hence a novel compensation method is proposed in this paper to avoid the wrong dead-time compensation.

If the current is less than 5% of the rated current, the dead-time compensation is not used. And if the current is in the interval from 5% to 20% of the rated current, the dead-time compensation value increases linearly with the output current increases. And the dead-time compensation reaches the rated

compensation value until the current is 20% of the rated current. Then the impact of the dead zone on the control is limited to the maximum extent.

### III. EXPERIMENTAL RESULTS

The tested motor is the 25kW IPMSM , TABLE 1 shows its parameters.

TABLE I. THE MOTOR PARAMETERS OF THE TEST

Name	Symbol	Parameter
Rated Power	$P$	25kW
Rated Current	$I$	46A
Poles	$p_n$	6
Rated frequency	$f$	195Hz
d-axis inductance	$L_d$	0.577mH
q-axis inductance	$L_q$	1.411mH
Stator resistance	$R_s$	0.062Ω
Back EMF	$u_s$	345V
Flux	$\Psi_m$	0.229 Vs
Viscous friction coefficient	$K_f$	0.005
Inertia	$J$	0.005

Fig. 5 shows the motor run with no load. Current is about 3% of the rated current, it is small and stable.

Fig. 6 shows the wave of full load when it is electric operation mode , and Fig 7 shows the wave of full load when it is generate mode. From 0 speed to 100% speed, they are all stable.

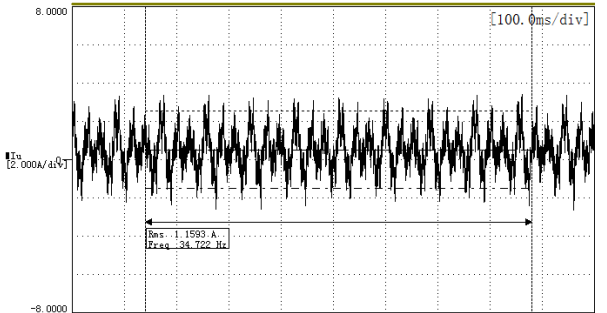


Fig. 4. No-load current of the V/f control.

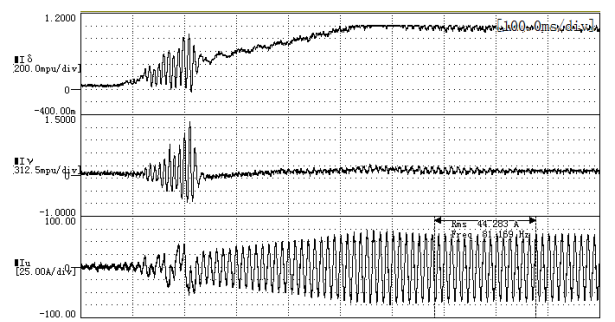


Fig. 5. Full-load currents(Motor mode).

Fig. 8 shows the comparison between the currents without efficient control and with efficient control at the same load. And Table 2 shows the value of two figures. Obviously, the currents of efficient control are smaller than those without efficient control. Therefore, the system efficiency of the efficient control is higher.

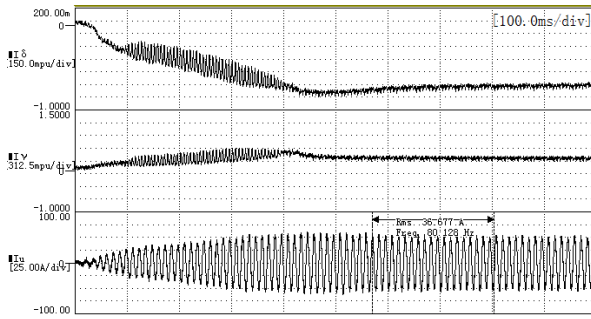


Fig. 6. Full-load current(Generate mode).

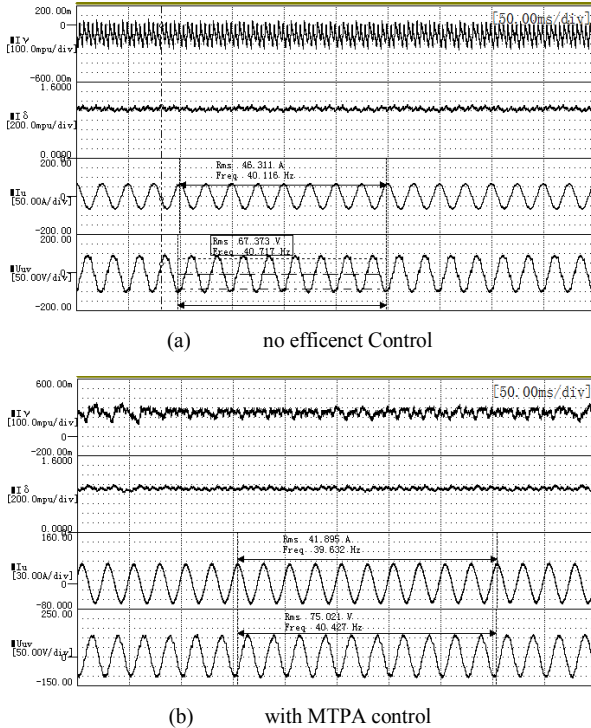


Fig. 7. Corporation of efficiency between no efficient Control and MTPA control.

TABLE II. OUTPUT DATES OF TWO CONTROL METHODS

Output	No Efficient control	MTPA control
$U_{wv}$ (V)	67.373	75.021
$I_u$ (A)	46.311	41.051
Power (kW)	5.404	5.334

#### IV. CONCLUSIONS

The theoretical analysis and experimental results show that the open-loop V/f control of PMSM is unstable. The proposed speed closed-loop is able to make the system stable. And the proposed reactive closed-loop improves the efficiency of the system. The experimental results show that the proposed V/f control method is stable and of high efficiency.

The proposed V/f control for PMSM avoids the extra cost and the reduced reliability caused by the rotor position sensor, and it is excellent in many industrial applications.

#### V. REFERENCES

- [1] P.D.C. Perera; F.Blaabjerg; J.K.Pedersen; P.Thogersen, "A sensorless, stable V/f control method for permanent-magnet synchronous motor drives," IEEE Transactions on Industry Applications. 2003, Vol.39(3), pp.783-791.
- [2] Seyed Hesam Jafari; Keith A.Corzine; Jing Huang, "Efficiency optimization of a sensorless V/f control method for PMSM," 3rd IEEE International Symposium on Sensorless Control for Electrical Drives, (SLED 2012). 2012, pp. 1-5.
- [3] R.Ancuti; I. Boldea; G.D. Andreescu, "Sensorless V/f control of high-speed surface permanent magnet synchronous motor drives with two novel stabilizing loops for fast dynamics and robustness," IET Electric Power Applications. 2010, Vol.4(3), pp. 149-157.
- [4] Sorin-Cristian Agarlita; Cristina-Elena Coman; Gheorghe-Daniel Andreescu; Ion Boldea, "Stable V/f control system with controlled power factor angle for permanent magnet synchronous motor drives," IET Electric Power Applications. 2013, Vol.7(4), pp. 278-286.
- [5] Gheorghe-Daniel Andreescu; Cristina-Elena Coman; Ana Moldovan; Ion Boldea, "Stable V/f control system with unity power factor for PMSM drives," 13th International Conference on Optimization of Electrical and Electronic Equipment (OPTIM). 2012, pp. 432-438.
- [6] Kai Yang; Xingxing Yang; Hongqin Xie; Yang Liu; Yingli Zhang; Xubiao Wei, Stable Sensorless V/f and  $\cos\phi=1$  Control for Permanent Magnet Synchronous Motor Drives. 17th International Conference on Electrical Machines and Systems (ICEMS), 2014: 3564 – 3568.
- [7] J.I.Itoh; N.Nomura; H. Ohsawa, "A Comparison between V/F Control and Position-Sensorless Vector Control for the Permanent Magnet Synchronous Motor," Proc. of the Power Conversion Conference PCC Osaka. 2002, Vol. 3, pp. 1310-1315.
- [8] Jun-ichi Itoh; Yuki Nakajima; Masakazu Kato, "Maximum Torque per Ampere Control Method for IPM Synchronous Motor based on V/f Control," IEEE 10th International Conference on Power Electronics and Drive Systems (PEDS). 2013, pp. 1322 - 1327
- [9] Shinn-Ming Sue; Tsai-Wang Hung; Jenn-Horng Liaw; Yen-Fang Li; Chen-Yu Sun, "A new MTPA control strategy for sensorless V/f controlled PMSM drives," 6th IEEE Conference on Industrial Electronics and Applications. 2011, pp. 1840 – 1844.
- [10] Zhuangyao Tang; Xiong Li; Serkan Dusmez; Bilal Akin, "A New V/f-Based Sensorless MTPA Control for IPMSM Drives," IEEE Transactions on Power Electronics. 2016, Volume: 31(6), pp. 4400 – 4415.
- [11] Zhuangyao Tang; Bilal Akin, "A robust V/f based sensorless MTPA control strategy for IPM drives," IEEE Applied Power Electronics Conference and Exposition (APEC). 2015, pp. 1575 – 1581